

THE INFLUENCE OF FLOW DISTRIBUTION ON THE PERFORMANCE IMPROVEMENT OF ELECTROSTATIC PRECIPITATOR

S M E HAQUE^{1*}, M G RASUL², A DEEV¹, M M K KHAN² and J ZHOU³

¹Process Engineering & Light Metals (PELM) Centre,
Faculty of Sciences, Engineering and Health
Central Queensland University
Gladstone, Queensland 4680
AUSTRALIA

²School of Advanced Technologies and Processes
Faculty of Sciences, Engineering and Health
Central Queensland University
Rockhampton, Queensland 4702
AUSTRALIA

³Stanwell Corporation Limited, Capricorn Highway via Gracemere
Queensland 4702
AUSTRALIA

*Corresponding author: Email: s.haque@cqu.edu.au

ABSTRACT

Particulate matter emission is one of the major air pollution problems of coal fired power plants. Though fine particles constitute a smaller fraction by weight of the total suspended particle matter in typical particle emissions, they are considered potentially hazardous to health because of their high probability of deposition in deeper parts of the respiratory tract. Electrostatic precipitators (ESP) are the most common, effective and reliable particulate control devices which can handle large gas volumes with a wide range of inlet temperatures, pressures, dust volumes and acid gas conditions. Though the electrostatic precipitators are generally running at the collection efficiency as high as 99.95%, the anticipated regulations on particulate matters of 2.5 microns (PM_{2.5}) have led the local power station to explore improvement options to further control the emissions of the fine particulate at a minimum cost even its current particulates emissions are well under the limits of its current environmental license. The performance of Electrostatic Precipitator (ESP) is significantly affected by its complex flow distribution. In this study the gas flow through the ESP at a local power station is modelled numerically using computational fluid dynamics (CFD) code Fluent to give insight to the flow behavior inside the ESP. The flow simulation was performed using the Realizable k-e model. The results of the simulation are discussed and compared with on-site measured data supplied by the power plant.

INTRODUCTION

The flow distribution within the ESP has been reported to have varying effects on its capture performance of fly ash particles depending on the size and arrangement of an ESP. It has been extremely difficult to fully evaluate the flow impact on individual ESP performance until CFD becomes available. CFD plays an ever increasing important role in predicting the flow field characteristics and particle trajectories inside the ESP and optimizing flow distributions within ESP by simulating proposed modification, which ensure that the required flow profiles are achieved – thus substantially reducing the outage time. However there is a limited research found in the literature for the prediction of turbulent flow behavior inside the ESP. Most of them used standard k-e turbulence model. Schwab and Johnson (1994) developed a numerical flow model of an ESP but did not create any physical geometry for the collection plates. They assumed flow resistance to represent the geometry. Varonos *et al.* (2002) developed a model which takes into account of the electric-field properties and the particle dynamics along with the basic fluid flow. They introduced flow resistance instead of creating any physical collecting plates. Bottner and Sommerfeld (2001) assumed in their model that particle charge was not varying with particle size or particle residence time. Gan and Riffat (1997) predicted the pressures loss coefficient of orifice and perforated plates. But the hole sizes in the plate are not specifically modeled rather they simplified the perforated plate with a plate of square holes of the same free area ratio. A laboratory scale ESP developed by Nikas *et al.* (2005) gave emphasis on the impact of the ionic wind on the gas flow. Dumont and Mudry (2003) made a comparative study on flow simulation results from different precipitator CFD models with actual field measurements of velocity patterns.

Although the above researches have been broadly dedicated to simulate fluid flow inside the ESP, no research has been attempted to simulate fluid flow for a full scale ESP considering all the physical details. The present study attempts to describe a detailed numerical method and an approach adopted to predict the flow pattern inside a full scale ESP. The predicted flow distributions are compared with the on-site measured data. It is to be noted that all the collecting electrodes (CE) are taken into account in this three dimensional model and have not been replaced by any equivalent resistance coefficient as other researchers have done in their studies. The induction of actual CE plates provides an important means to assess the practical impact of these critical components inside the ESP and have the potential to provide improvement in design and maintenance activities.

GEOMETRY OF ESP

The power station in this study has 4 power generating units of 350 MW capacity each. Each unit has 2 single-stage, plate-type, rigid-frame, cold-side and dry ESPs which are called as pass A and pass B. Each pass has two streamlines covering 4 zones. The effective length, width and height of each casing are 30.36 m, 22 m and 13.1 m respectively. The width and height of the CE walls are 5.76 m and 12.5 m respectively. Each CE wall is made of 12 CE plates. Each pass has 54 passages having 400mm CE wall spacing. Discharge electrodes (DE) are welded into pipe frames with 2 frames per passage. The width of DE frame is 5.76m and the heights are 5 m and 7.5 m. Dust removal method for both collection electrodes and discharge electrodes is rapping. Three perforated plates are located within the inlet evase to establish good fluid flow distribution inside the ESP. One outlet screen is located within the outlet evase. Due to the symmetry in geometry the numerical model is constructed to represent only one-half of a pass. Figure 1 shows the geometrical representation of the plant ESP.

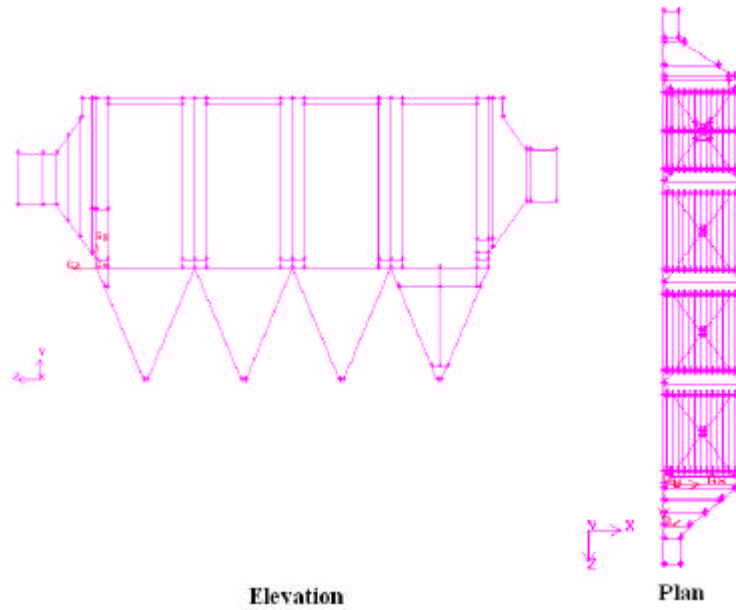


Figure 1: ESP configuration

NUMERICAL APPROACH

Numerical computation of fluid transport includes conservation of mass, momentum and energy, chemical species concentration and turbulence models. Gambit is used as a preprocessor to create the geometry, discretize the fluid domain into small cells to form a volume mesh or grid and set up the appropriate boundary conditions. The flow properties are then specified and the problems are solved and analyzed by Fluent solver.

The basis of modeling of an incompressible Newtonian fluid flow module is the use of the conservation of mass equations (Munson *et al.* 2002).

$$\frac{\partial \mathbf{r}}{\partial t} + \vec{\nabla} \cdot (\mathbf{r}\vec{V}) = 0 \quad (1)$$

and the momentum equation (Munson *et al.* 2002)

$$\frac{\partial \vec{V}}{\partial t} + \vec{V} \cdot \vec{\nabla} \vec{V} = -\frac{\vec{\nabla} p}{\rho} + \mathbf{n} \vec{\nabla}^2 \vec{V} + \vec{g} \quad (2)$$

Where ρ is the fluid density and \mathbf{n} is the kinematic viscosity of the fluid. The pressure and velocity gradients are denoted as $\vec{\nabla} p$ and $\vec{V} \cdot \vec{\nabla} \vec{V}$ respectively. For the turbulent flow inside the ESP, the key to the success of CFD lies with the accurate description of the turbulent behavior of the flow. To model the turbulent flow in an ESP, there are a number of turbulence models available in Fluent. The realizable k-e model is a relatively recent development and differs from the standard k-e model in two important ways. The realizable k-e model contains a new formulation for the turbulent viscosity and a new transport equation for the dissipation rate, ϵ , which has been derived from an exact equation for the transport of the mean-square vorticity fluctuation (Fluent Inc, 2005).

A source term is added to the k-e equation for the pressure drop across the perforated plates. In the CFD simulation, the perforated plates are modeled as thin porous media of finite thickness with directional permeability over which the pressure change is defined as a combination of viscous loss term and an inertial loss term which is given by

$$\Delta p = -\left(\frac{\mu}{a}v + C_2 \frac{1}{2}rv^2\right)\Delta m \quad (3)$$

Where μ is the laminar fluid viscosity, a is the permeability of the plate, C_2 is the pressure loss coefficient per unit thickness of the plate, v is the velocity normal to the porous face and Δm is the thickness of the plate. A separate CFD study was done placing a small piece of the original perforated plate which is shown in Fig. 2 inside a round duct to find the effect of viscous loss term in Eq. 3 at turbulent flow condition.

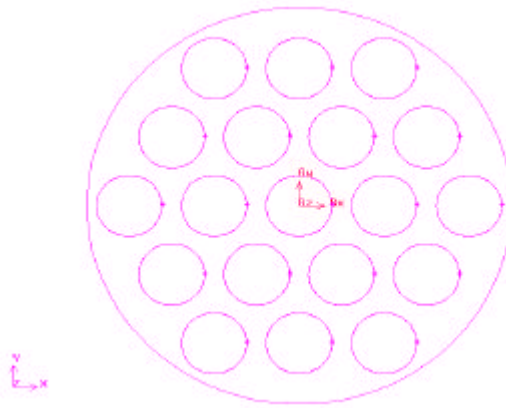


Figure 2: Perforated plate configuration

The finite volume methods have been used to discretize the partial differential equations of the model using the simple method for pressure–velocity coupling and the first order upwind scheme to interpolate the variables on the surface of the control volume. The segregated solution algorithm was selected. Non equilibrium wall functions were applied for near wall treatment purpose. The input parameters for the inlet were inlet velocity, turbulence intensity and hydraulic diameter. The CFD simulation was performed with a Pentium IV 1.8 GHz 32bit CPU workstation with 2GB RAM-memory and 18GB hard disc memory.

RESULTS AND DISCUSSIONS

The operating conditions used for the numerical model are based upon available test data taken by Dattner and Donaldson (1992) at inlet and outlet duct and inside the collection chamber with the unit offline and the ID fans operating. A windmill vane type anemometer was used to measure the velocity at different planes inside the casing. Measurement of the velocity inside the ESP was carried out for the velocity of 9.36 m/s at an average temperature of 24⁰ C at plane 1 as is shown in Fig. 3 which is set as inlet velocity of the CFD model. To obtain a fully developed turbulent flow inside the ESP using the outflow boundary condition, the outlet is placed far from the outlet evase as is shown in Fig. 4. The total number of nodes of the ESP model of this study is 553058.

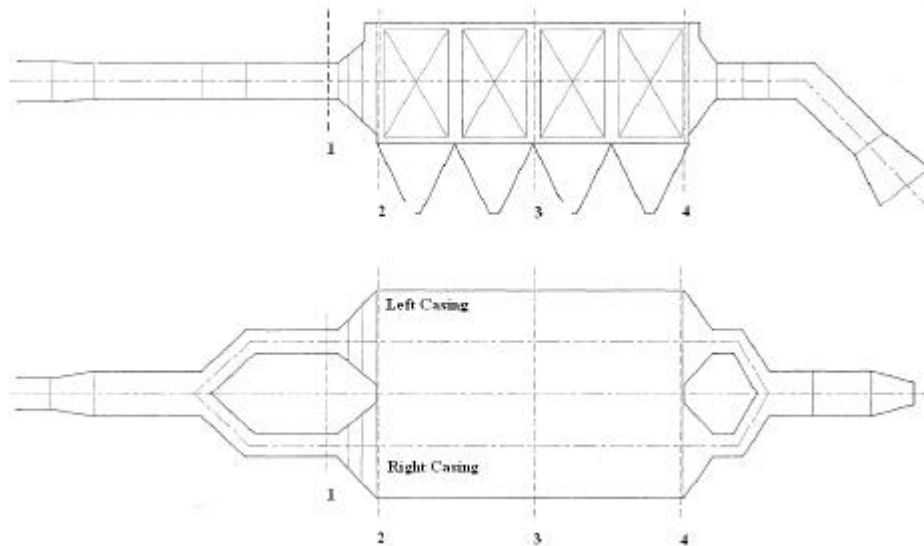


Figure 3: Measurement planes for velocity distribution

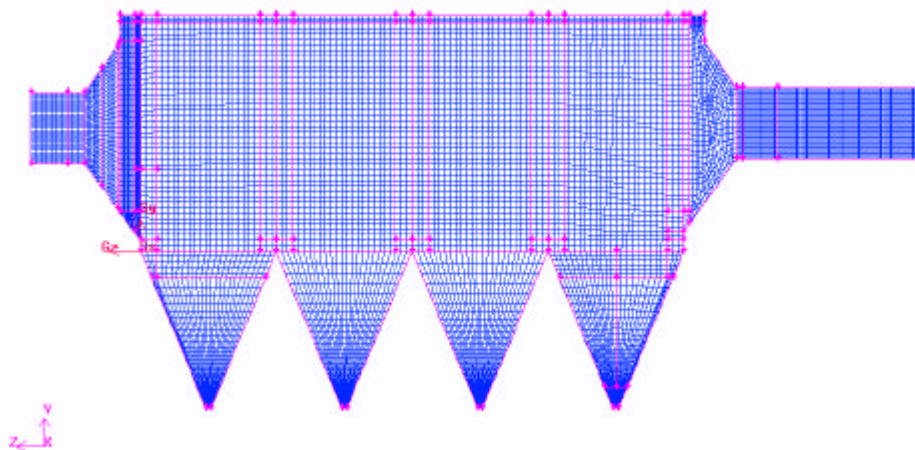


Figure 4: Numerical grid for ESP

Three perforated plates with the thickness of 8 mm, 2 mm and 2 mm are located inside the inlet evase. Figure 5 represents the predicted pressure drop across the 8 mm thick perforated plate at different velocities for air and for an imaginable gas with 100 times lesser viscosity than air. Since the change of gas viscosity by the factor of 100 did not result in any measurable difference in the predicted pressure drop, it has been concluded that the pressure drop across the perforated plate is mainly due to the inertial loss at turbulent flow condition. Appropriate values for C_2 are then calculated from the handbook (Idelchik, 1994).

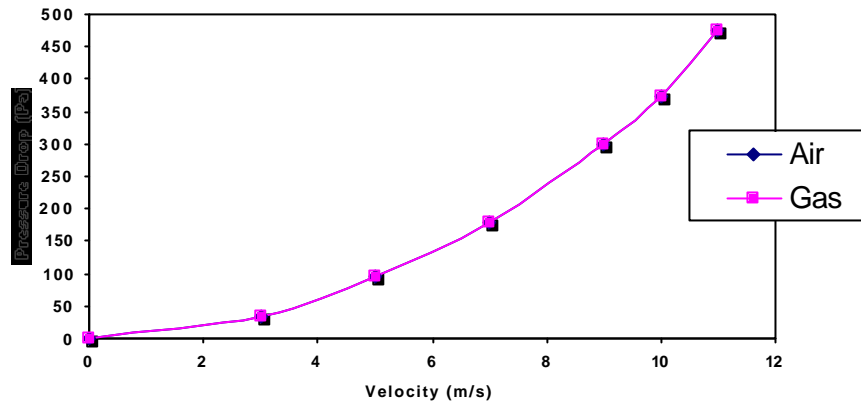


Figure 5: Pressure drops at different velocities for air and gas

The lower part of the third perforated plate, which is known as distribution wall differs with the geometry from the upper part. Two simulations have been carried out with and without introducing the distribution wall. The results that have been found without introducing the distribution wall are presented in Figures 6 and 7. The predicted velocity at height $y=11.8$ m of plane 2, 3 and 4, shown in Fig. 3 are compared with the measured velocity. Figures 8, 9 and 10 present the velocity comparison at three measurement planes, which give a reasonably good prediction with a maximum deviation of about 20% on the measured values. The velocity distributions shown in Figures 6 and 7 were found non-uniform. Figures 11 and 12 present the velocity profiles after introducing the distribution wall in the model. The results show that the flow is more uniformly distributed while using the distribution wall. The predicted velocity at plane 2 is then compared with the available on-site data which is shown in Fig. 13. The prediction was found satisfactory with minor deviation from the measured data. The discrepancy may be associated with the course mesh size near the wall and lack of details of the exact geometry in the model. More simulation is being carried out with finer mesh in order to achieve a better prediction at near wall region. It is expected that these will lead to a better match with the measured values and provide a good insight to the flow behavior inside the ESP.

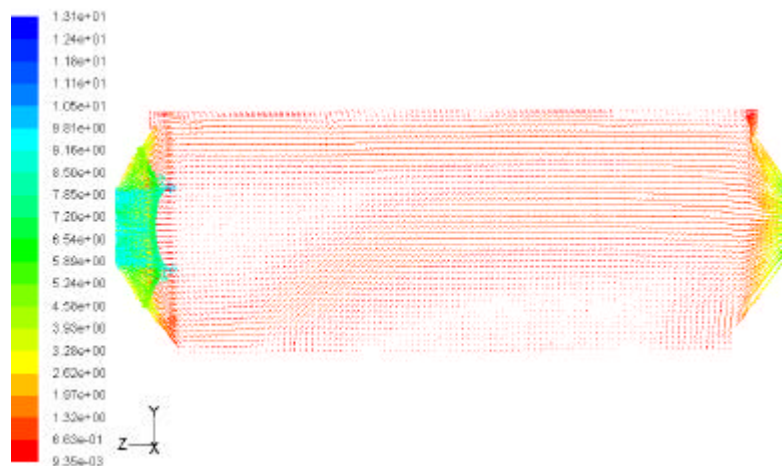


Figure 6: Velocity distribution at $x=0$ m (symmetry plane) – side view section

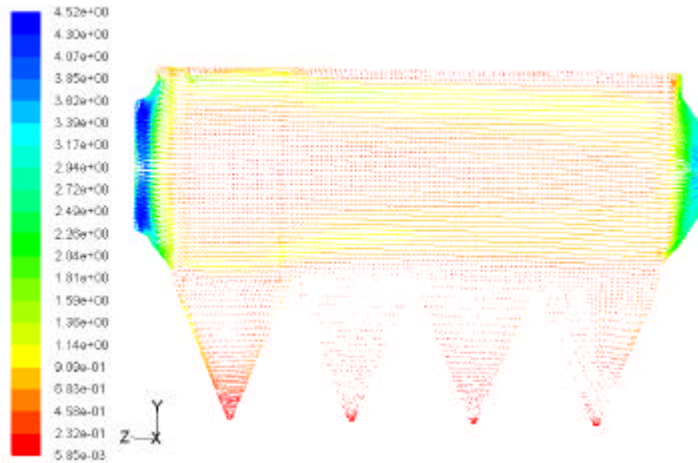


Figure 7: Velocity distribution at $x=2.75\text{ m}$ – side view section

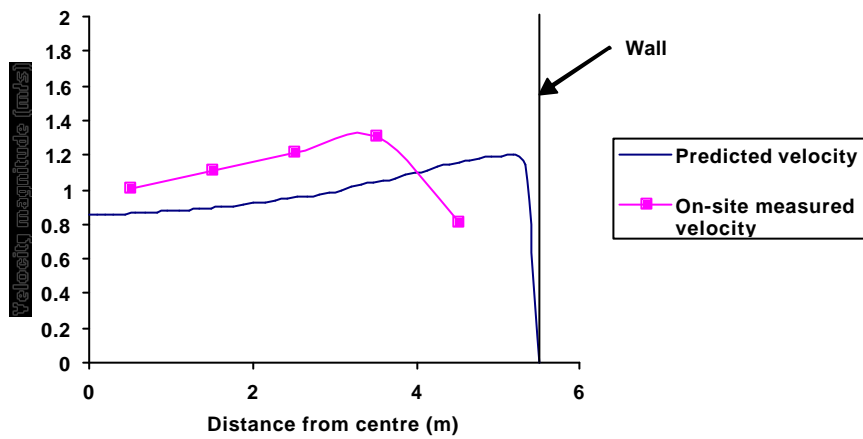


Figure 8: Velocity magnitude at $y=11.8\text{ m}$ (Plane 2). Comparison between the measured data and CFD prediction

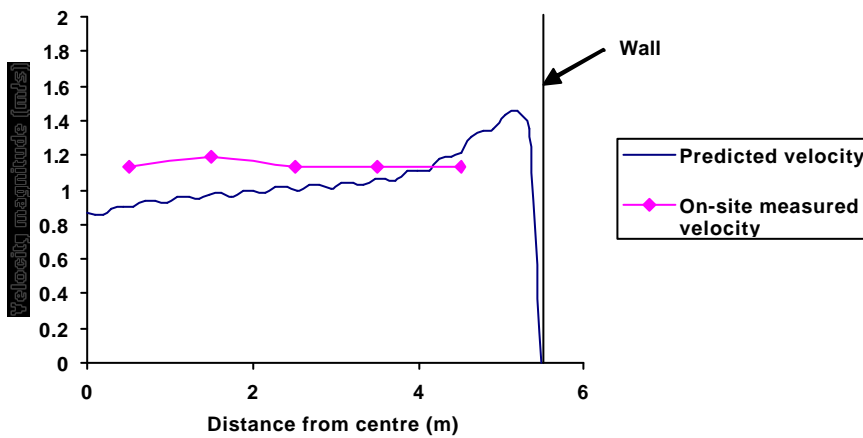


Figure 9: Velocity magnitude at $y=11.8\text{ m}$ (Plane 3). Comparison between the measured data and CFD prediction

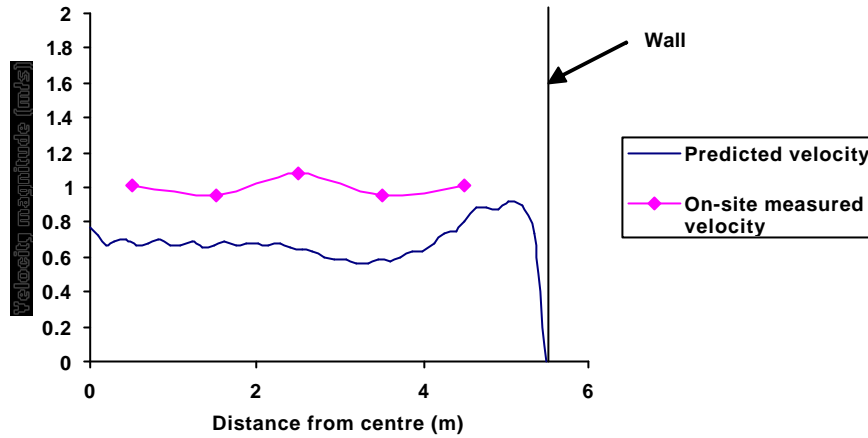


Figure 10: Velocity magnitude at $y=11.8$ m (Plane 4). Comparison between the measured data and CFD prediction

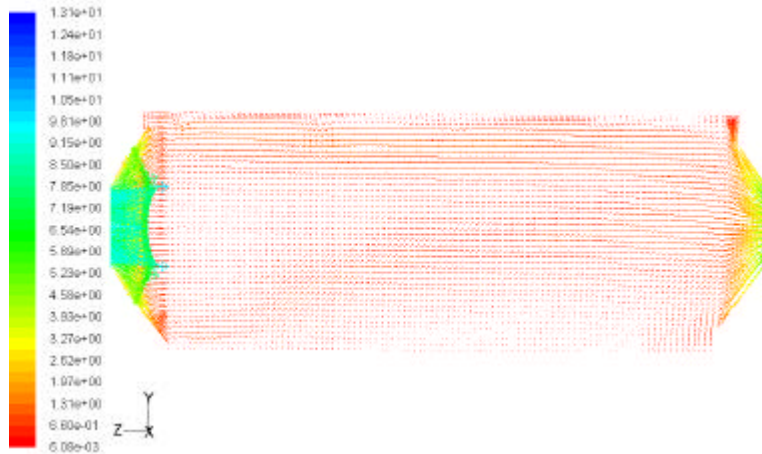


Figure 11: Velocity distribution at $x=0$ m (symmetry plane) using the distribution wall. side view section

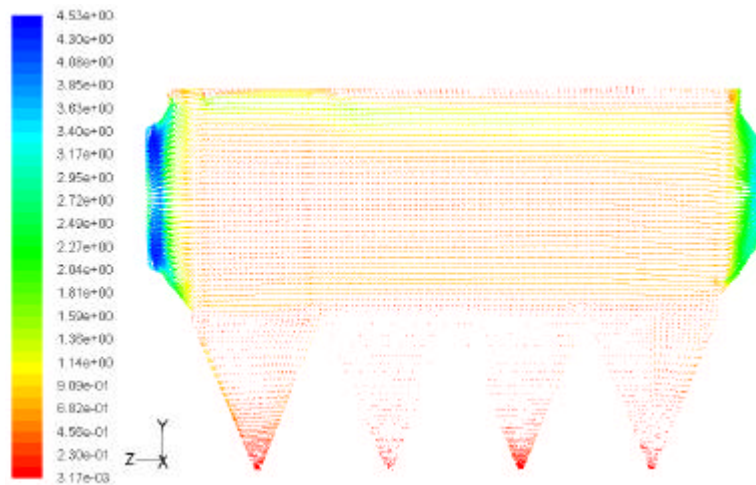


Figure 12: Velocity magnitude at $y=11.8$ m (Plane 2). Comparison between the measured data and CFD prediction using the distribution wall

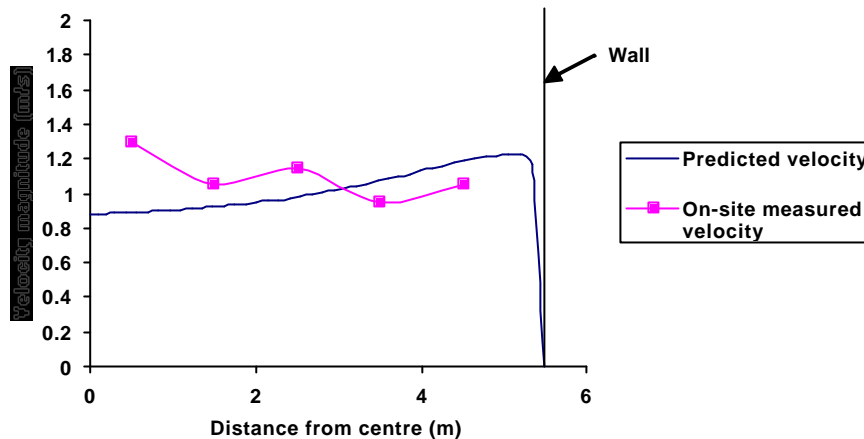


Figure 13: Velocity magnitude at $y=11.8$ m (Plane 4).

Comparison between the measured data and CFD prediction using the distribution wall

CONCLUDING REMARKS

An on going CFD analysis for the full scale ESP is presented. The collecting electrodes are modeled in their actual condition. Realizable k-e model for turbulence condition inside the ESP is applied. Numerically predicted velocities inside the ESP are compared with the measured data. As seen, these predictions are not the exact matches with the measured data. The deviations may be due to the course mesh near the wall, lack of details of exact geometry in the model, incorrect pressure jump coefficient of the porous plates. The inclusion of actual CE plates in the model is expected to provide direct means to assess the performance of these critical components inside ESP and have the potential to show future improvement in designs. Further simulation is being carried out introducing finer mesh near the wall and different pressure jump coefficient of distribution wall in order to achieve an optimized flow distribution inside the ESP and thus improve its performance. Moreover, particle size distribution inside the ESP will be analyzed to explore the interaction of varying sized particles with flue gas. Study of such two-phase three dimensional flow under a charged confined space may give a good prediction on the effects of flow distribution on the particle residence time inside the ESP. This model can be useful in identifying options on operation and maintenance improvement activities by ESP tuning, optimizing flow distribution, field charging and rapping cycles and necessary plant modifications.

ACKNOWLEDGEMENTS

The authors would like to thank Stanwell Corporation Limited for supporting this work and providing on-site measured data.

REFERENCES

- Bottner C.U. and Sommerfeld M. (2001). Euler/Lagrange calculations of particle motion in turbulent flow coupled with an electric field, Proceedings of ECCOMAS Computational Fluid Dynamics Conference, 2001.
- Dumont B. J. and Mudry R. G. (2003). Computational fluid dynamic modeling of electrostatic precipitators, Proceedings of Electric power conference, 2003.

Dattner R. and Donaldson I. (1992). Gas distribution measurement report, Stanwell Power Station, 1992.

Fluent Inc. (2005). Fluent 6.2 User's Guide, 2005.

Gan, G. and Riffat S. B. (1997). Pressure loss characteristics of orifice and perforated plates, *Experimental Thermal and Fluid Science*, **14**, 160-165, 1997.

Idelchik I. E. (1994). Handbook of hydraulic resistance, 3rd edition, CRC Press Inc., 1994.

Munson B. R., Young, D. F. and Okiishi, T. H. (2002). Fundamentals of fluid mechanics, 4th ed., John Wiley & Sons Inc., NY, 2002.

Nikas K. S. P., Varnos A. A. and Bergeles G. C. (2005). Numerical simulation of the flow and the collection mechanisms inside a laboratory scale electrostatic precipitator, *Journal of Electrostatics*, **63**, 423-443, 2005.

Schwab, M. J. and Johnson R. W. (1994). Numerical design method for improving gas distribution within electrostatic precipitators, *Proceedings of the American Power Conference*, **56**, 882-888, 1994.

Varonos A. A., Anagnostopoulos J. S. and Bergeles G. C. (2002). Prediction of the cleaning efficiency of an electrostatic precipitator, *Journal of Electrostatics*, **55**, 111 – 133, 2002